



This paper is a part of the hereunder thematic dossier published in OGST Journal, Vol. 70, No. 6, pp. 909-1132 and available online [here](#)

Cet article fait partie du dossier thématique ci-dessous publié dans la revue OGST, Vol. 70, n°6, pp. 909-1132 et téléchargeable [ici](#)

Oil & Gas Science and Technology – Rev. IFP Energies nouvelles, Vol. 70 (2015), No. 6, pp. 909-1132

Copyright © 2015, IFP Energies nouvelles

- 909 > *Editorial - Enhanced Oil Recovery (EOR), Asphaltenes and Hydrates*
Éditorial - EOR «récupération assistée de pétrole», Asphaltes et Hydrates
D. Langevin and F. Baudin

ENHANCED OIL RECOVERY (EOR)

- 917 > *HP-HT Drilling Mud Based on Environmentally-Friendly Fluorinated Chemicals*
Boues de forage HP/HT à base de composés fluorés respectueux de l'environnement
I. Henaut, D. Pasquier, S. Rovinetti and B. Espagne
- 931 > *Effective Viscosity in Porous Media and Applicable Limitations for Polymer Flooding of an Associative Polymer*
Viscosité effective dans des médias poreux et limites d'application de l'injection de polymères associatifs
P. Zhang, Y. Wang, Y. Yang, W. Chen and S. Bai
- 941 > *Dynamic Gelation of HPAM/Cr(III) under Shear in an Agitator and Porous Media*
Gélification dynamique de HPAM/Cr(III) sous cisaillement dans un agitateur et en milieu poreux
Y. Haiyang, W. Yefei, Z. Jian, L. Peng and S. Shenglong
- 951 > *Computer Modeling of the Displacement Behavior of Carbon Dioxide in Undersaturated Oil Reservoirs*
Modélisation par ordinateur du comportement de déplacement du dioxyde de carbone dans des réservoirs d'huile non saturés
B. Ju, Y.-S. Wu and J. Qin
- 967 > *Predicting CO₂ Minimum Miscibility Pressure (MMP) Using Alternating Conditional Expectation (ACE) Algorithm*
Prédiction de la pression miscibilité minimum (MMP) du CO₂ en utilisant un algorithme basé sur l'ACE (Alternating Conditional Expectation)
O. Alomair, A. Malallah, A. Elsharkawy and M. Iqbal
- 983 > *Towards the Development of Bitumen Carbonates: An Integrated Analysis of Grosmont Steam Pilots*
Vers le développement des carbonates bitumineux : une analyse intégrée des pilotes vapeur de Grosmont
C.C. Ezeuko, J. Wang, M.S. Kallos and I.D. Gates
- 1007 > *A Novel Model of Foam Flooding Considering Multi-Factors for Enhancing Oil Recovery*
Un nouveau modèle d'injection de mousse considérant de multiples facteurs afin d'améliorer la récupération de pétrole
J. Wang, H. Liu, H. Zhang, G. Zhang, P. Liu and K. Sepehrnoori

- 1025 > *Testing of Snorre Field Foam Assisted Water Alternating Gas (FAWAG) Performance in New Foam Screening Model*
Vérification des performances de la méthode FAWAG (Foam Assisted Water Alternating Gas) sur le champ de Snorre, en Norvège, avec un nouveau modèle de sélection des mousses
P. Spirov and S. Rudyk

ASPHALTENES

- 1035 > *Structural Study of Asphaltenes from Iranian Heavy Crude Oil*
Étude structurale d'asphaltes de pétrole brut lourd iranien
L. Davarpanah, F. Vahabzadeh and A. Dermanaki
- 1051 > *Experimental Study and Mathematical Modeling of Asphaltene Deposition Mechanism in Core Samples*
Étude expérimentale et modélisation mathématique du mécanisme de dépôt d'asphalène dans des carottes de forage
T. Jafari Behbahani, C. Ghotbi, V. Taghikhani and A. Shahrabadi
- 1075 > *Prediction of the Gas Injection Effect on the Asphaltene Phase Envelope*
Prévision de l'effet d'injection de gaz sur l'enveloppe de phase des asphaltes
P. Bahrami, R. Kharrat, S. Mahdavi and H. Firoozinia

HYDRATES

- 1087 > *Methane Hydrate Formation and Dissociation in the Presence of Silica Sand and Bentonite Clay*
Formation et dissociation d'hydrates de méthane en présence de sable de silice et d'argile de bentonite
V. Kumar Saw, G. Udayabhanu, A. Mandal and S. Laik
- 1101 > *Prediction of Mass Flow Rate in Supersonic Natural Gas Processing*
Prédiction du débit massique dans les applications de traitement supersonique du gaz naturel
C. Wen, X. Cao, Y. Yang and Y. Feng
- 1111 > *Experimental Study on Hydrate Induction Time of Gas-Saturated Water-in-Oil Emulsion using a High-Pressure Flow Loop*
Étude expérimentale sur le temps d'induction d'hydrate d'une émulsion eau-huile saturée en gaz en utilisant une boucle à circulation sous haute pression
X.F. Lv, B.H. Shi, Y. Wang, Y.X. Tang, L.Y. Wang and J. Gong
- 1125 > *Hollow Silica: A Novel Material for Methane Storage*
La silice creuse : un nouveau matériau pour le stockage de méthane
V.D. Chari, P.S.R. Prasad and S.R. Murthy

A Novel Model of Foam Flooding Considering Multi-Factors for Enhancing Oil Recovery

J. Wang^{1,2*}, H. Liu¹, H. Zhang¹, G. Zhang³, P. Liu⁴ and K. Sepehrnoori²

¹ MOE Key Laboratory of Petroleum Engineering in China University of Petroleum, Beijing 102249 - China

² Department of Petroleum & Geosystems Engineering, The University of Texas at Austin, Austin 78712 - USA

³ CNOOC Tianjin Branch Company, Tianjin 300452 - China

⁴ Sinopec Shengli Oilfield Branch Company, Shandong Dongying 257000 - China

e-mail: wangjing8510@163.com

* Corresponding author

Abstract — Foam flooding is a promising technique for achieving mobility control and diverting fluid into low-permeability strata in post-water-flooding reservoirs. However, foam flow is very complicated and is influenced by many factors which have not been studied and explored very rigorously (i.e. permeability, surfactant concentration, foam quality, reservoir temperature, oil saturation, water saturation and seepage velocity). Based on core flooding experiments of foam flowing and blocking rules using two kinds of foaming agents, a novel model of foam flooding considering the influences of the above factors is established and solved using a reservoir simulator which is formulated using the IMPES method in conjunction with a Runge-Kutta method. Then, the validation is performed by core flooding experiments in both the absence and presence of oil. Finally, the simulator is used to investigate the effects of the permeability max-min ratio, ratio of vertical to horizontal permeability, gas-liquid ratio, depositional sequence, foaming agent concentration, and reservoir temperature.

Résumé — Un nouveau modèle d'injection de mousse considérant de multiples facteurs afin d'améliorer la récupération de pétrole — L'injection de mousse est une technique prometteuse pour atteindre un contrôle de la mobilité et détourner le fluide dans des couches à faible perméabilité de réservoirs après injection d'eau. Toutefois, l'écoulement de mousse est très compliqué et est influencé par de nombreux facteurs qui n'ont pas été étudiés et explorés de manière très rigoureuse (à savoir la perméabilité, la concentration en tensioactif, la qualité de la mousse, la température du réservoir, la saturation en pétrole, la saturation en eau et la vitesse d'écoulement). Sur la base d'expériences d'injection de mousse dans des carottes et de règles de blocage en utilisant deux types d'agents moussants, un nouveau modèle d'injection de mousse qui tient compte des influences des facteurs ci-dessus est établi et résolu, en utilisant un simulateur de réservoir basé sur la méthode IMPES combinée à la méthode Runge-Kutta. Ensuite, la validation est réalisée par des expériences d'injection dans des carottes à la fois en l'absence et en présence de pétrole. Enfin, le simulateur est utilisé pour étudier les effets du rapport max/min de perméabilité, du rapport de perméabilité verticale/horizontale, du rapport gaz/liquide, des séquences de dépôt, de la concentration de l'agent moussant et de la température du réservoir.

INTRODUCTION

Foam flooding is an EOR (Enhance Oil Recovery) technique taking foam as the displacing fluid. Foam not only effectively decreases the mobility ratio of gas to oil but also weakens the phenomena of gas channeling and steam override [1, 2]. Moreover, due to the particular mechanisms of foam generation and collapse, foam presents the selective blocking features of “big block and small not block” and “water block and oil not block” when it flows in porous media [3], which is very favorable for enhancing oil recovery. In the past few years, foam flooding has been carried out in many pilots in China, and most of them have shown a good performance [4].

In a study of foam triggering mechanisms, Kovscek *et al.* [5] attributed triggering mechanisms of foam to increasing the viscosity of the driving phase; Rossen *et al.* [6] attributed the triggering mechanism to declining gas phase mobility; Kovscek and Bertin [7] reported that both increasing gas phase viscosity and decreasing the gas phase relative permeability take effect simultaneously, and hence they improved the models for foam viscosity and the gas phase relative permeability. However, it is controversial that relative permeability and viscosity are considered separately [8]. As can be seen from these studies, it is recognized that the triggering mechanism of a foam system is decreasing the gas mobility, but many different approaches, *e.g.* modifying the gas phase viscosity or gas phase relative permeability or modifying both the gas phase viscosity and relative permeability are considered to achieve this mechanism. Nevertheless, foam flow in porous media is a very complicated process, since the lamellae in the flowing state will increase the viscosity of the driving phase and the lamellae adsorbed on the pore surface will reduce gas relative permeability. Unfortunately, because of the surrounding environment, especially the properties of the rock and fluid, both mechanisms are difficult to distinguish and test by experiments. Therefore, the above approaches for representing foam mechanisms are partial and difficult to quantify. In this paper, the mobility of the gas phase is considered as a whole to test and be measured by the resistance factor. This method includes increasing the viscosity of the displacing phase as well as decreasing the gas relative permeability, avoids repeated tests, and takes into account the effects of these two mechanisms. Numerical simulation is a technique to study the flow characteristics described by mathematical models [9]. It has features of low cost, high efficiency and good repeatability, and can demonstrate the entire complex flow process. Because foam is a very complex system where gas is the dispersed phase and liquid is the continuous phase, accurate prediction is difficult. There are

several approaches to deal with its complexity. The first approach is called “population balance”, which quantifies the relation between foam mobility and foam texture and all the mechanisms of creation and destruction of liquid films, or lamellae [10-13]. It uses a differential equation to represent foam texture *in situ*, but the basic concept is consistent with the local-equilibrium version, in which foam texture is an algebraic function of local conditions [6]. In all population balance models, the rate of creation of lamellae depends on gas velocity through pore throats where snap-off takes place [10-13]. The second approach represents foam mobility as an empirical function of many influence factors [14-17]. The third approach is the “fixed- P_c^* model”, which relies on the relation between capillary pressure, foam texture and foam mobility [18]. In essence, it is also a local-equilibrium version of the population balance for strong foams under conditions where capillary pressure dominates foam texture and gas mobility [6]. The first approach is more complex, and there is no way to separate the effects of lamella generation and destruction in history-matching coreflood results [6]; the second approach is simple, but it disregards the relation between foam mobility and texture; the third approach is between the other two, but it disregards the foam strength influenced by many key factors. Based on the advantages and disadvantages of the above three models, a synthesized multi-factor foam model is presented. In the novel model, the foam generation depends on the critical gas velocity, which is a function of the aqueous phase mobility fraction [12]. The foam collapse depends on limiting capillary pressure, at which foam collapses abruptly [19]. Since S_w is related to P_c through the capillary-pressure function $P_c(S_w)$, this means that foam remains at a given water saturation $S_w^* \equiv S_w(P_c^*)$. Foam strength, which is influenced by permeability, surfactant concentration, foam quality, reservoir temperature and oil saturation, affects the foam mobility, which is evaluated by the foam resistance factor. Therefore, a foam resistance factor model derived from our coreflood experiments using two kinds of foam agents is used to represent foam strength features [20]. The advantages of this approach reflect the competing goals of simplicity and completeness; however, the model is not able to describe slow generation or destruction processes thoroughly, considering the influence of flow velocity on foam mobility.

Finally, the model validation was performed by core flooding experiments; the factors which affect the EOR effects of foam flooding were investigated using the novel model: the permeability max-min ratio, the ratio of vertical to horizontal permeability, gas-water ratio, foaming agent concentration, temperature and depositional sequence.

1 GOVERNING EQUATION

1.1 Mass Conservation Equations

The assumptions imposed on the flow equations include:

- four components: oil, water, gas and surfactant;
- gas, water and surfactant generate foam which reduces the gas mobility;
- the whole process is isothermal, and the energy transfer is neglected;
- fluid flow obeys the generalized Darcy's law;
- phase equilibrium is reached instantaneously;
- foam only affects mobility (the ratio of gas relative permeability to viscosity).

Mass balance equation for the oil phase:

$$\nabla \cdot \left(\frac{\vec{k}k_{ro}}{\mu_o B_o} \nabla \Phi_o \right) + q_o = \frac{\partial}{\partial t} \left(\frac{\phi S_o}{B_o} \right) \quad (1)$$

Mass balance equation for the aqueous phase:

$$\nabla \cdot \left(\frac{\vec{k}k_{rw}}{\mu_w B_w} \nabla \Phi_w \right) + q_w = \frac{\partial}{\partial t} \left(\frac{\phi S_w}{B_w} \right) \quad (2)$$

Mass balance equation for the gas phase:

$$\nabla \cdot \left(\frac{\vec{k}k_{rg}}{\mu_g B_g R_g} \nabla \Phi_g \right) + q_g = \frac{\partial}{\partial t} \left(\frac{\phi S_g}{B_g} \right) \quad (3)$$

Mass balance equation for the surfactant (foaming agent):

$$\begin{aligned} -\nabla \cdot (c_s \vec{v}_w) + \nabla \cdot (\vec{d}_s \phi S_w \nabla c_s) \\ + q_w c_s = \frac{\partial(\phi S_w c_s)}{\partial t} + \frac{\partial[\rho_r(1-\phi)\hat{c}_s]}{\partial t} \end{aligned} \quad (4)$$

In which k is the absolute permeability, μm^2 ; k_{rl} is the relative permeability of phase l ; μ_l is the effective viscosity of phase l , $\text{mPa}\cdot\text{s}$; B_l is the formation volume factor of phase l , m^3/m^3 ; ∇ is the divergence operator; q_l is the source and sink for phase l , $\text{m}^3/(\text{day}\cdot\text{m}^3)$; R_g is the gas resistance factor; Φ_l is the potential of phase l , MPa ; S_l is the saturation of phase l ; ϕ is porosity; c_s is the surfactant concentration, kg/m^3 ; d_s is the diffusion coefficient of the surfactant, m^2/s ; ρ_r is the rock density, kg/m^3 ; \hat{c}_s is the adsorption concentration of the surfactant, kg/kg .

1.2 Auxiliary Equations

Let S_w , S_o and S_g be water, oil and gas saturation, respectively. Then the saturation constraint equation is:

$$S_o + S_w + S_g = 1 \quad (5)$$

Also, p_w , p_o and p_g are water, oil and gas phase pressures, respectively; the capillary pressure equations are:

$$p_{cow} = p_o - p_w \quad (6)$$

$$p_{cgo} = p_g - p_o \quad (7)$$

In which p_{cow} is the capillary pressure between oil and water, Pa; and p_{cgo} is the capillary pressure between gas and oil, Pa.

1.3 Process Mechanism Models of Foam Flooding

1.3.1 Foam Resistance Factor

The effects of different factors on foam block characteristics are obtained by experiments using two kinds of surfactants. One is sodium dodecyl sulfate (#1) and another is an industrial foaming agent used in the Henan oilfield (#2). Then, a range of variograms and their correction models are applied to fit the relationship linking the foam resistance factor and other factors. The undetermined coefficients can be obtained using DATAFIT software [21] based on experimental results. Because of the consistency in physical meaning among variograms, the foam generation and collapse mechanisms, this method evades the defect from the conventional mathematical regression method that can merely be applied to a local scale but not to the extended area.

Resistance Factor vs Foaming Agent Concentration

A logistic model is a straightforward model used to forecast the population growth and presents an ‘‘S’’ tendency which can be divided into elementary, acceleration, transfer, deceleration and saturation periods. The adsorbance of active molecules on the gas/liquid interface has a similar trend, which determines the variation of foam blocking ability. As a result, the blocking capacity increases as the surfactant concentration increases, although there is a break in the curve at about 0.5% by weight. Based on experimental results (Fig. 1) and the Critical Micelle Concentration (CMC) introduced as a characteristic parameter, a logistic function was used to model the relationship between the resistance factor and foaming agent concentration:

$$R_f(c_s) = \frac{R_f|_{c_s=CMC}}{1 + a \cdot \exp(-r \cdot c_s)} \quad (8)$$

Using DATAFIT and the above model, the undetermined coefficients were obtained. For surfactant #1,

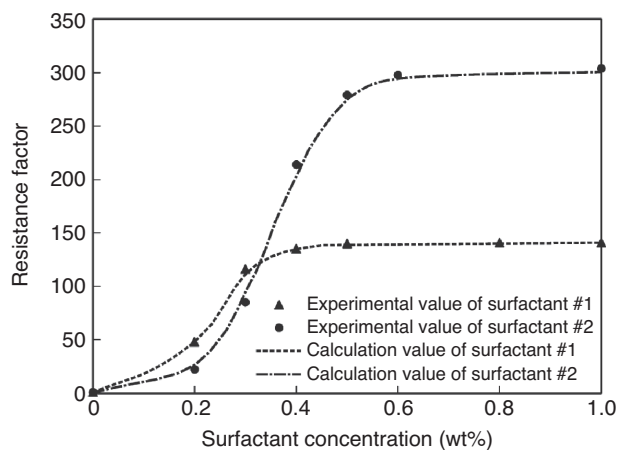


Figure 1

Comparison between experiments and the model of the resistance factor for different surfactant concentrations.

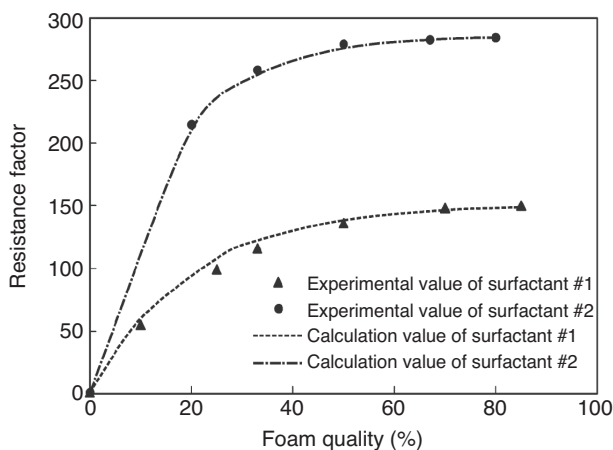


Figure 2

Comparison of experiments and the model of the resistance factor for different foam qualities.

$a_1 = 100$ and $r_1 = 19.5$; and for surfactant #2, $a_2 = 230$ and $r_2 = 16$.

Resistance Factor vs Foam Quality

Khatib *et al.* [19] showed that at a given gas flow rate, the foam resistance factor increases slightly with increasing foam quality ranging from 50% to 98%. De Vries and Wit [22] reported that at an imposed total flow rate, the foam resistance factor increases as foam quality increases until the break point; beyond that it decreases. Chang and Grigg [23] found that the foam resistance factor increases with increasing foam quality ranging from 33.3% to 80%. We found that the resistance factor first increases and then decreases as the foam quality increases, and the break point is at about 80%. However, it is challenging for the foam quality to reach above 80% in foam flooding pilots. Hence, the proportional region between the resistance factor and foam quality is of concern from the practical application viewpoint. Derived from the data of this region (Fig. 2), the variation resembles the exponential variogram model. After deliberating the endpoint feature, the relationship between the resistance factor and foam quality is:

$$R_f(\eta) = 1 + R_f|_{\eta=\eta_c} \cdot \left[1 - \exp\left(-\frac{3\eta}{b}\right) \right] \quad (9)$$

Using DATAFIT and the above model, the undetermined coefficients were obtained. For surfactant #1, $b_1 = 60$; and for surfactant #2, $b_2 = 45$.

Resistance Factor vs Permeability

One merit of the foam used for EOR is “big block and not small block”, meaning foam has a better blocking ability in high-permeability regions or layers and the blocking ability nearly disappears in low-permeability regions or layers. This indicates shear thinning of the foam, which has been experimentally confirmed by many researchers [24-28]. In order to characterize the relation between the resistance factor and permeability (Fig. 3), dimensionless permeability (k_D) is used. The relation between the resistance factor and dimensionless permeability is:

$$R_f(k) = R_f|_{k=k_c} \cdot \left[1 - \frac{1 - k_D}{1 + m(k_D)^n} \right] \quad (10)$$

$$k_D = k/k_c \quad (11)$$

Using DATAFIT and the above model, the undetermined coefficients were obtained. For surfactant #1, $m_1 = 3$ and $n_1 = 2$; and for surfactant #2, $m_2 = 8.5$ and $n_2 = 1.05$.

Resistance Factor vs Temperature

Influencing mechanisms of temperature on foam resistance are diverse [29]. First of all, the dissolving capacity increases as the temperature increases, so the adsorbance of active molecules on the gas/liquid interface decreases,

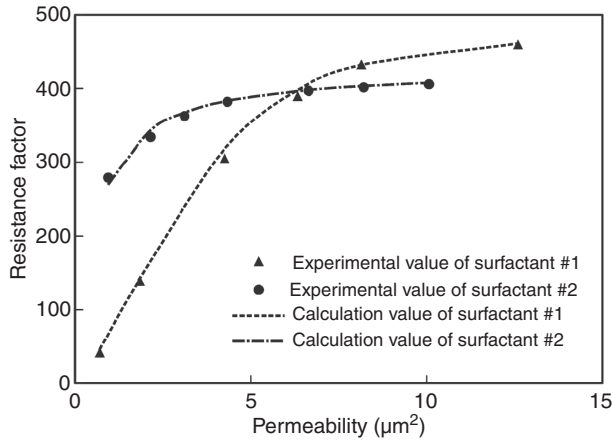


Figure 3
Comparison of experiments and the model of the resistance factor for different permeabilities.

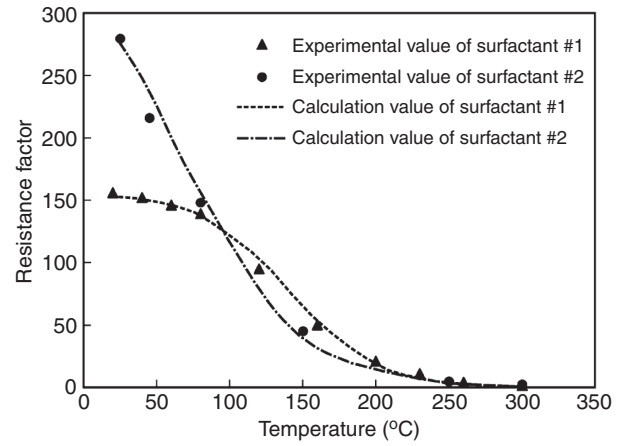


Figure 4
Comparison of experiments and the model of the resistance factor for different temperatures.

which results in a decrease in the strength of the lamellae. In addition, an increase in temperature will accelerate the drainage rate of liquid from lamellae to the liquid phase and promotes the collapse and coalescence of the bubbles. Moreover, an increase in temperature will also speed up the degradation of the foaming agent. Friedmann *et al.* [12] and Maini and Ma [30] reported that the foam resistance ability largely decreases as the temperature increases in porous media. Based on experimental results and the break point denoted as T_r (Fig. 4), the relation between temperature and foam quality is modeled as:

$$R_f(T) = \frac{R_f|_{T=T_r}}{1 + \exp\left(\frac{T-\alpha}{\beta}\right)} \quad (12)$$

Using DATAFIT and the above model, the undetermined coefficients were obtained. For surfactant #1, $\alpha_1=140$ and $\beta_1=30$; for surfactant #2, $\alpha_2=70$ and $\beta_2=38$.

Resistance Factor vs Oil Saturation

The mechanisms by which oil affects the foam stability are diverse. Some studies have confirmed that the foam can be generated in the presence of oil by selecting appropriate foaming agents [31-34]. Some studies have stated that foam can be generated when the oil saturation is below a critical value [35-37], but some other studies have shown that foam is generated at relatively high oil saturation [34, 38, 39]. The characteristics of foaming

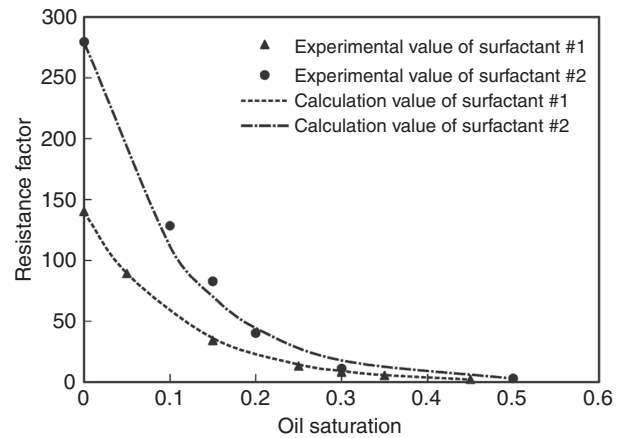


Figure 5
Comparison of experiments and the model of the resistance factor for different oil saturation ratios.

agents and oil samples used in the experiments may cause these differences. In general, it is commonly agreed that the presence of oil is detrimental to the foam stability [35, 36, 38, 40], and our experimental results also support this view. Therefore, oil saturation is more likely to be regarded as an influencing factor of the resistance factor than a critical condition of foam collapse. Based on experimental results (Fig. 5), the foam resistance factor exponentially decreases as the oil saturation increases, and different values of c will be achieved for different foaming agents and oil samples:

$$R_f(S_o) = R_f|_{S_o=0} \cdot \exp(-c \cdot S_o) \quad (13)$$

Using DATAFIT and the above model, the undetermined coefficients were obtained. For surfactant #1, $c_1 = 9.0$; for surfactant #2, $c_2 = 9.2$.

Seepage Velocity - The Critical Generation Condition of Foam

The generation mechanisms of foam in porous media include lamellae snap-off, lamellae lag and lamellae trapping. Many experiments indicated that the lamellae snap-off or lamellae flow will not occur until the pressure or velocity overpasses the critical value. In fact, it is a triggering mechanism. Once foam is in place, velocity can be reduced, but the foam remains. Fridmann *et al.* [12] found that the critical velocity increases as the liquid volume fraction decreases according to the following:

$$v_{gc} = \frac{1.52}{V_L^{-1.54}} \quad (14)$$

where v_{gc} is the critical velocity of foam generation, m/day, and V_L is the mobility fraction of the aqueous phase.

Water Saturation - The Critical Collapse Condition of Foam

Based on the DLVO theory [41, 42], the collapse of foam is related to critical capillary force. When the practical capillary force exceeds the critical value, foam will collapse. However, the capillary force is a function of water saturation; the higher the water saturation, the smaller the capillary force will be. Therefore, once the water saturation is lower than the critical value corresponding to the critical capillary force, the foam will collapse. Khatib *et al.* [19] found that the critical capillary force logarithmically decreases as the permeability and gas velocity increase, which also reflects the shear-thinning characteristics of the foam system. Based on the definition of the Leverett J-function and the empirical relation of the Leverett J-function [43, 44], we have:

$$J(S_w^*) = \frac{P_c^*}{\sigma_{gw} \cos \theta} \sqrt{\frac{k}{\phi}} = a_J \left(\frac{S_w^* - S_{wc}}{1 - S_{wc}} \right)^{b_J} \quad (15)$$

Khatib *et al.* [19] also found that the critical capillary pressure logarithmically decreases with increasing permeability (may reflect the effect of the pore structure) and gas velocity, which also reflects the shear-thinning characteristic of foam:

$$P_c^*(k, v_g) = -a_1 \ln(kv_g) + b_1 \quad (16)$$

Substituting Equation (16) into Equation (15), the limiting water saturation was obtained to be:

$$S_w^* = (1 - S_{wc}) \left[\frac{-a_1 \ln(kv_g) + b_1}{a_J \sigma_{gw} \cos \theta} \sqrt{\frac{k}{\phi}} \right]^{1/b_J} + S_{wc} \quad (17)$$

In Equations (15-17), $J(S_w^*)$ is the J function; P_c^* is the critical capillary force, MPa; v_g is the gas velocity, cm/s; σ_{gw} is the gas-water interfacial tension, mN/m; θ is the wetting angle; a_1 , b_1 , a_J and b_J are undetermined coefficients; S_w^* is the critical water saturation.

Multi-factor Gas Mobility Model

Based on a previous study [6], the resistance factor of the gas phase in porous media with the presence of foam is:

$$R_g = \begin{cases} 1 & S_w \leq (S_w^* - \varepsilon) \text{ and } v < v_{gc} \\ 1 + \frac{(R_{kf} - 1)(S_w - S_w^* + \varepsilon)}{2\varepsilon} & (S_w^* - \varepsilon) < S_w < (S_w^* + \varepsilon) \text{ and } v \geq v_{gc} \\ R_{kf} & S_w \geq (S_w^* + \varepsilon) \text{ and } v \geq v_{gc} \end{cases} \quad (18)$$

where ε is a special parameter; $\varepsilon = 0.001$ was used in this paper. It will not affect the simulation of the displacement effect. It is only used to avoid the jump of the calculated gas mobility due to the actual water saturation fluctuation above and below the critical value. The influencing factors of foam blocking ability in the process of foam flooding are numerous, and play a role simultaneously, hence it is very valuable to quantitatively characterize the foam resistance factor under multiple scenarios. Also, it is beneficial to the advancement of numerical simulation technology of foam flooding. Therefore, a novel foam resistance factor model that comprehensively considers the influences of the above factors is achieved:

$$R_{kf}(c_s, \eta, k, T, S_o) = A_r R_f|_{k=k_c} \frac{\left[1 - \frac{1-k_D}{1+m(k_D)^m} \right] \cdot \left[1 - \exp\left(-\frac{3\eta}{b}\right) \right] \cdot \exp(-c \cdot S_o)}{\left[1 + a \cdot \exp(-r \cdot c_s) \right] \cdot \left[1 + \exp\left(\frac{T-g}{\beta}\right) \right]} \quad (19)$$

$$A_r = \frac{R_f|_{c_s=CMC} \cdot R_f|_{\eta=\eta_c} \cdot R_f|_{T=T_r} \cdot R_f|_{S_o=0}}{R_f|_{Test}^4} \quad (20)$$

The validation of the multi-factor gas mobility model can be verified by the experimental data, which is shown in Figure 6. The values of the undetermined coefficients are shown in Table 1.

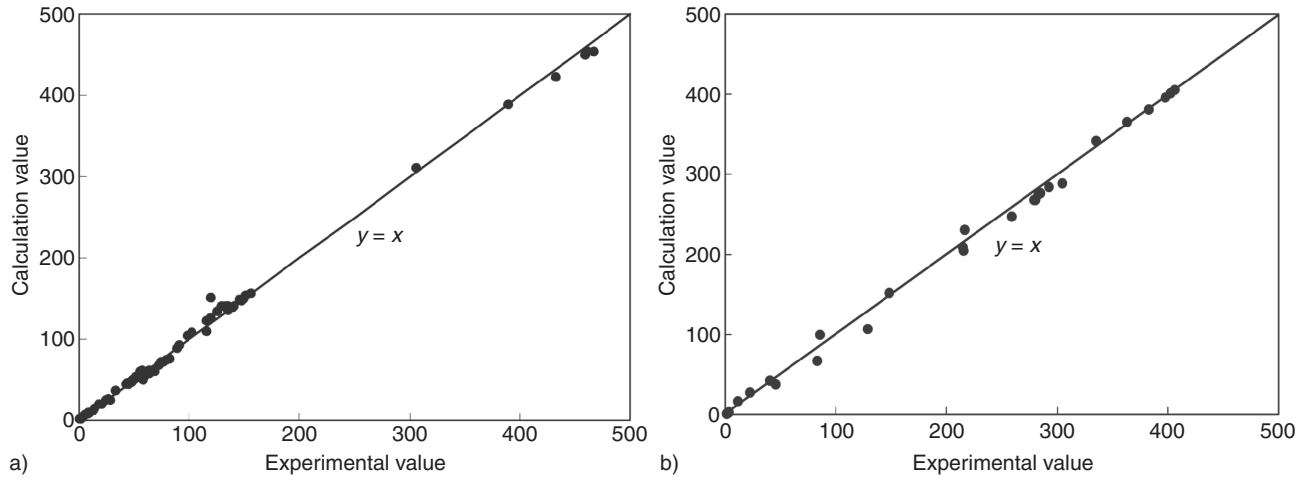


Figure 6

Validation of the multi-factor gas mobility model using experimental data. a) Surfactant #1, b) Surfactant #2.

Equation (19) not only comprehensively considers the influences of the rock properties, fluid properties and surroundings on foam block characteristics, but also avoids the discontinuous behavior of gas mobility caused by the critical foaming agent concentration and critical oil saturation, which will greatly improve the stability of the numerical simulation process.

Correction of the Resistance Factor for Weak Foam

It was reported that flow resistance is small and foam textures are coarse, consistent with the injection of unfoamed gas or weak foam in the inlet region, and there exists a strong foam piston-like front moving through the porous media [6, 44]. This phenomenon has also been verified by many experiments [45, 46]. However, most of the existing foam flow models cannot simulate this process [6]. In this model, the above resistance factor model is based on strong foam, so the following correction function is introduced to represent this effect:

$$R_f(L) = \frac{R_{kf}^0}{1 + AA \cdot \exp(-RR \cdot L)} \quad (21)$$

where R_{kf}^0 is the resistance factor of strong foam; L is the flow distance of weak foam or unfoamed gas and foaming agent solution, m; AA and RR are model coefficients.

1.3.2 Adsorption Model for the Surfactant

The adsorption of the foaming agent will occur when it flows in the porous media and obeys the typical Langmuir law:

$$\hat{c}_s = \hat{c}_{smax} \frac{b_s c_s}{1 + b_s c_s} \quad (22)$$

where b_s is the Langmuir parameter, $(\text{kg}/\text{m}^3)^{-1}$; \hat{c}_{smax} is the maximum adsorbed concentration, kg/kg .

1.3.3 Capillary Desaturation and Interfacial Tension Model

The foaming agent can also reduce the oil-water interfacial tension by its surfactant characteristics and decrease the residual oil saturation [47]:

$$S_{or} = S_{ormin} + \frac{S_{ormax} - S_{ormin}}{1 + A_N N_{co}} \quad (23)$$

$$N_{co} = \frac{\mu_w v_w}{\sigma_{wo}} \quad (24)$$

$$\sigma_{wo} = a_\sigma \times 10^{-b_\sigma c_s} \quad (25)$$

where N_{co} is the capillary number; σ_{ow} is the oil-water interfacial tension, mN/m ; S_{ormin} is the limit of residual oil saturation under a high capillary number; S_{ormax} is the residual oil saturation under a low capillary number; a_σ , b_σ and A_N are undetermined coefficients.

TABLE 1
Values of undetermined coefficients

Surfactant #1													
<i>a</i>	<i>r</i>	<i>b</i>	<i>m</i>	<i>n</i>	α	β	<i>c</i>	$R_{f _{\text{Test}}}$	$R_{f _{c=CMC}}$	$R_{f _{\eta=\eta_0}}$	$R_{f _{T=T_r}}$	$R_{f _{S_o=0}}$	$R_{f _{k=k_c}}$
100	19.5	60	3	2	140	30	9.0	139	139	156	150	139	430
Surfactant #2													
<i>a</i>	<i>r</i>	<i>b</i>	<i>m</i>	<i>n</i>	α	β	<i>c</i>	$R_{f _{\text{Test}}}$	$R_{f _{c=CMC}}$	$R_{f _{\eta=\eta_0}}$	$R_{f _{T=T_r}}$	$R_{f _{S_o=0}}$	$R_{f _{k=k_c}}$
230	16	45	8.5	1.05	70	38	9.2	279	300	285	360	279	390

1.3.4 Relative Permeability Model

The Stone II model is used to calculate the three-phase relative permeability [48]:

$$k_{rw} = k_{rwo} \left[\frac{S_w - S_{wc}}{1 - S_{wc} - S_{orw}} \right]^{n_w} \quad (26)$$

$$k_{row} = k_{rocw} \left[\frac{1 - S_w - S_{orw}}{1 - S_{wc} - S_{orw}} \right]^{n_{ow}} \quad (27)$$

$$k_{rog} = k_{rocw} \left[\frac{1 - S_{wc} - S_{org} - S_g}{1 - S_{wc} - S_{org}} \right]^{n_{og}} \quad (28)$$

$$k_{rg} = k_{rgr} \left[\frac{S_g - S_{gc}}{1 - S_{wc} - S_{org} - S_{gc}} \right]^{n_g} \quad (29)$$

$$k_{ro} = f_3(S_w, S_g) = k_{rocw} \left[\left(\frac{k_{row}}{k_{rocw}} + k_{rw} \right) \times \left(\frac{k_{rog}}{k_{rocw}} + k_{rg} \right) - k_{rw} - k_{rg} \right] \quad (30)$$

where k_{rocw} is the oil phase relative permeability corresponding to connate water; k_{rw} and k_{rg} are the water and gas phase relative permeability, respectively; k_{row} and k_{rog} are the oil phase relative permeability in the oil-water system and oil-gas system, respectively; n_w , n_{ow} , n_w , n_{og} and n_g are input parameters; S_{wc} , S_{orw} , S_{gc} and S_{org} are the end-points in oil-water and oil-gas systems' relative permeability functions.

1.3.5 Physical Properties of the Gas Phase [49]

The formation volume factor is:

$$B_g = 3.458 \times 10^{-4} \times Z \times \frac{273 + t}{p_g} \quad (31)$$

The expansion factor is:

$$E_g = \frac{1}{B_g} = 2891.7 \times \frac{p_g}{Z(273 + t)} \quad (32)$$

where Z is the compressibility factor; t is the reservoir temperature, °C.

1.3.6 Capillary Pressure Model

Capillary pressure is a function of saturation:

$$p_{cow}(S_w) = A_1 \cdot \sqrt{\frac{\phi}{k}} \cdot \left(\frac{S_w - S_{wc}}{1 - S_{wc} - S_{or}} \right)^{B_1} \quad (33)$$

$$p_{cgo}(S_g) = A_2 \cdot \sqrt{\frac{\phi}{k}} \cdot \left(\frac{S_g - S_{gc}}{1 - S_{gc} - S_{or}} \right)^{B_2} \quad (34)$$

where A_1 and A_2 are input parameters; B_1 and B_2 are capillary pressure exponents.

2 SOLUTION AND VALIDATION OF THE MATHEMATICAL MODEL

2.1 Solution Method

In this model, gas flow velocity is used as the triggering mechanism; water saturation obtained based on DLVO theory is used for the bubble collapse mechanism. If foam exists in the porous media, the foaming agent concentration, foam quality, permeability, temperature and oil saturation come into play for calculating the resistance factor in the grid. This method avoids solving the foam population balance equation. A method for solving this mathematical model is as follows:

- the IMPES (Implicite Pressure Explicite Saturation) method is used to solve the pressure and saturation equations to obtain the pressure and saturation distributions for each phase;
- the classical four-order Runge-Kutta method is applied to solve the concentration equation of the foaming agent;
- the local gas flow velocity, critical gas flow velocity and critical water saturation based on the grid pressure and saturation are solved;

TABLE 2
Parameter values for simulations of Kovscek's experiment

a	r	b	m	n	α	β	A_r
100	19.5	60	8	1.1	140	30	2.0
$R_{f k=kc}$	a_J	b_J	a_1	b_1	AA	RR	
1 200	1.3	-0.9	0.1	1.5	80	40	

- the critical generation condition and critical collapse condition are used to determine whether there is foam in the grid. If foam exists in the grid, using permeability, the foaming agent concentration, gas-liquid ratio, temperature and oil saturation are used to calculate the resistance factor; otherwise, the resistance factor is set to one;
- then the resistance factor will be substituted into the gas flow equation;
- repeat steps (1-5) until the end of the simulation time.

2.2 Validation of the Novel Model

In the Absence of Oil

The model includes all mechanisms that are:

- crucial to the process;
- known with reasonable accuracy.

With the purpose of validating the model, the foam flow data obtained from Kovscek [44] is used. Core and fluid data are based on reference [44], and other model parameters are listed in Table 2. The fitting result of the multi-factor model shown in Figure 7 is a slightly better fit than the population balance model although

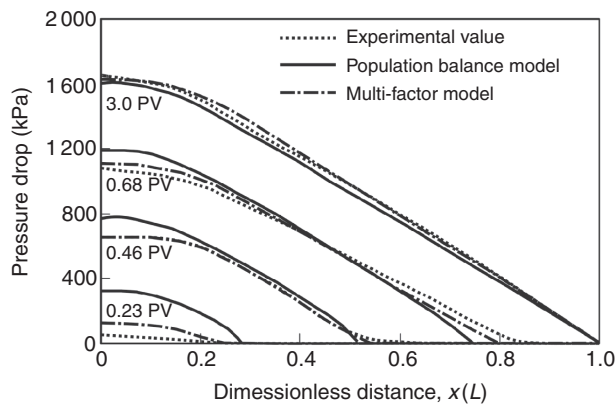


Figure 7

Comparison between the computed value using the multi-factor model, Kovscek's coreflood data, and the computed value using a population balance model

the curve for 0.23 PV is not a close fit due to the lack of strong foam and gas channeling.

In the Presence of Oil

Because the impact of oil presence is considered, one group of foam flooding experimental data is also used. In this experiment, foaming agent solution (SDS: surfactant #1) with the concentration of 0.4 wt% was injected continuously into linear unconsolidated media of length 0.3 m at a rate of 2 mL/min, while gas was also injected continuously to give a foam quality of 80% at the sandpack entrance. The permeability is $4.5 \mu\text{m}^2$ and porosity is 0.33. The initial oil saturation is 0.4 and oil viscosity is about 2.0 mPa·s. At 120 min, continued water flooding was performed at a rate of 5mL/min. Other model parameters are listed in Table 3. The comparison between computed and experimental data is shown in Figure 8 and the agreement is excellent.

3 RESULTS AND DISCUSSION

In order to study thoroughly the differences between the foam flooding with the gas-water flooding and the influences of many parameters on the EOR effect, a synthetic geological model is built. The reservoir scale is $10 \times 10 \times 2$ with the dimensions of $dx = dy = 10$ m and $dz = 5$ m, as shown in Figure 9. The time step is 1 d. The reservoir temperature is 30°C and pressure is 20 MPa. The viscosity of oil is 20 mPa·s and initial oil saturation is 0.8. The porosity is 0.3, and the permeability is $1 \mu\text{m}^2$ and $4 \mu\text{m}^2$ for the top and bottom layers, respectively. The ratio of vertical permeability to horizontal permeability is 0.1. The production rate is 20 m³/day, with an injection-production ratio of 1:1. The foam is injected when the water-cut reaches 90% ($t = 2\ 000$ d) and the slug size is 0.4 PV. The foaming agent concentration is 0.5 wt% and the injection gas-water ratio is 1:1 in formation conditions. The gas viscosity is 0.03 mPa·s and the water viscosity is 1.0 mPa·s. The difference between gas-water flooding and foam flooding is that the foaming agent concentration equals zero or not. Other model parameters are listed in Table 4.

TABLE 3
Parameter values for simulations of the foam flooding experiment

a	r	b	m	n	α	β	c
100	19.5	60	3	2	140	30	9.0
A_r	$R_{f k=kc}$	a_J	b_J	a_1	b_1	AA	RR
2.5	430	1.3	-0.9	0.1	1.5	80	35

TABLE 4
Parameter values for simulations of foam flooding in a heterogeneous reservoir

a	r	b	m	n	α	β	c
100	19.5	60	3	2	140	30	9.0
A_r	$R_{f k=kc}$	a_J	b_J	a_1	b_1	AA	RR
2.0	500	1.3	-0.9	0.1	1.5	80	35

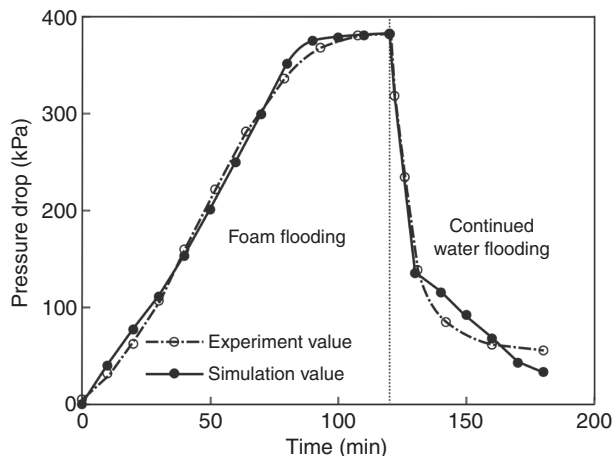


Figure 8

Comparison between computed and experimental pressure drop for foam flooding in oil-bearing conditions.

3.1 Comparing Foam Flooding with Water + Gas Flooding

Gas has a much smaller viscosity and lower density; therefore, if gas is used as the displacing fluid, gas channeling and override will occur. The major advantage of foam flooding is that the lamella of the foam can cut off the gas phase, effectively decrease the mobility ratio of gas to oil, and weaken the phenomena of gas channeling and override. Figure 10 shows the distribution of gas saturation at different times by foam flooding and water + gas flooding (the foam slug was injected between

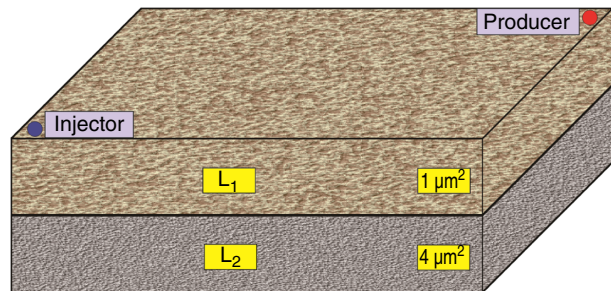


Figure 9

Geological model with vertical heterogeneity.

2 000 d and 2 600 d). It is clear that, when $t = 2 500$ d, the gas phase area of L_1 is larger than L_2 for both water + gas flooding and foam flooding; the gas saturation of water + gas flooding is lower than foam flooding, but the gas phase area is larger for both L_1 and L_2 ; the amount of gas in L_1 is more than L_2 for gas-water flooding, which is the reverse for foam flooding. One explanation is that in transgressive depositional sequence reservoirs [50], the fractional flow of bottom strata is larger; but when the gas is injected into the reservoir, the gas is inclined to enter the top strata because of gravitational differentiation. At the same time, the gas viscosity is much lower than both water and oil; thus, the gas flows fast in both lateral and vertical directions. However, if the gas exists in the form of foam, the gas mobility will greatly decrease. Thus, the gas flows slowly and the gas saturation is larger for foam flooding. With lower permeability and

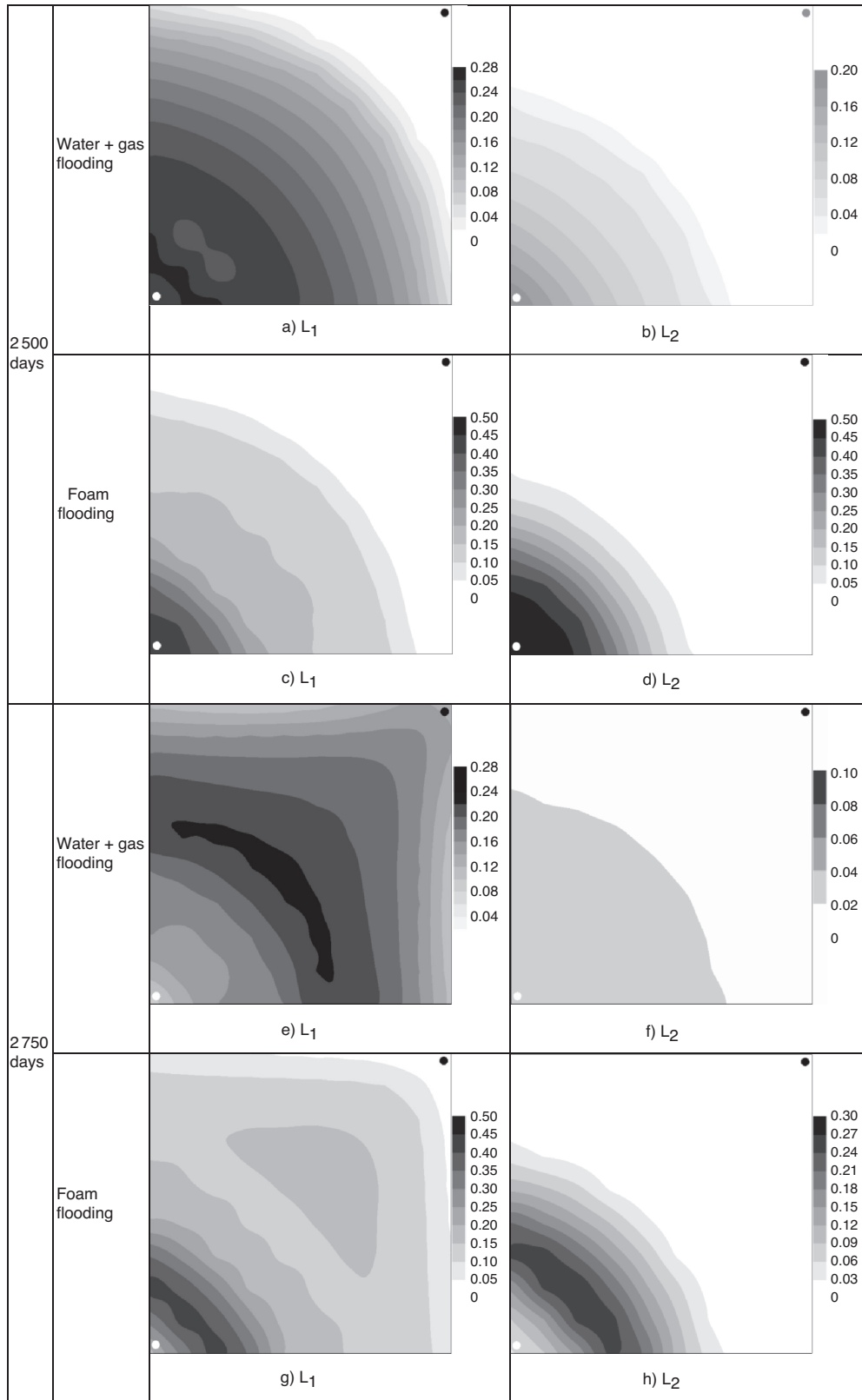


Figure 10
Distribution of gas saturation at different times by foam flooding and water + gas flooding.

higher oil saturation in L_1 , the resistance factor is lower, which results in the gas phase area being larger in L_1 . When $t = 2750$ d, the gas has already channeled to the producer along the L_1 , and the gas saturation is close to zero in the L_2 for water + gas flooding. Conversely, gas channeling does not appear and the gas saturation is still about 0.3 and exists in the form of foam in L_2 for foam flooding. The foam located in L_2 makes water divert into the lower-permeability strata (L_1) and displaces more additional remaining oil than water + gas flooding.

The development effects of different methods are shown in Figure 11. It is clear that the ultimate recovery order is foam flooding (48.8%) > water + gas flooding (46.7%) > water flooding (43.7%) and the flood-response time of

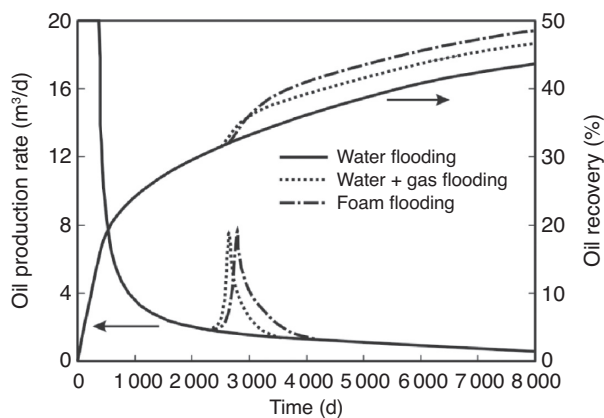


Figure 11

Development effects of different methods.

water + gas flooding is earlier and shorter than foam flooding because of the densities of water, oil and gas. Due to gravitational differentiation, both top and bottom layers are well swept by gas and water, so the ultimate recovery of water + gas flooding is larger than water flooding. In the foam flooding process, some of the unfoamed gas flows in the top layer to sweep the remaining oil, and some of the gas in the form of foam flows in the bottom layer. As previously analyzed, the blocking ability of foam in the high-permeability layer is stronger than in the low-permeability layer. As a result, the gas flows in the high-permeability layer the same as in the low-permeability layer, and more water enters the lower-permeability layer and consequently displaces more oil. Hence, foam can both effectively inhibit the gas override and establish a large flow resistance to realize the fluid diversion, which is favorable for enhancing oil recovery in heterogeneous reservoirs.

3.2 Sensitivity Analysis of Foam Flooding Enhancing Oil Recovery

In a lab study, foam flooding can enhance oil recovery by more than 20% in suitable conditions. Actually, most of the fields in China have carried out foam flooding and obtained satisfactory results [4], but the incremental oil recoveries are less than lab results due to their adverse conditions. Hence, studying the effects of reservoir and foam properties for choosing suitable reservoirs to perform foam flooding is very important. The permeability max-min ratio, ratio of vertical to horizontal permeability, depositional sequence, reservoir temperature, foam

TABLE 5
Parameters of simulated projects for sensitivity analysis

Influence factors	K_r	k_v/k_h	η (%)	Sequence	Concentration (wt%)	Temperature (°C)
K_r	2, 4, 6, 8, 10, 12, 15	0.1	50	Transgressive	0.5	30
k_v/k_h	4	0.01, 0.05, 0.1, 0.5, 1.0	50	Transgressive	0.5	30
η	4	0.1	20, 25, 33, 40, 50, 66, 75, 80, 90	Transgressive	0.5	30
Depositional sequence	4	0.1	50	Transgressive, regressive	0.5	30
Foaming agent concentration	4	0.1	50	Transgressive	0.1, 0.2, 0.3, 0.4, 0.5, 0.6, 1.0	30
Reservoir temperature	4	0.1	50	Transgressive	0.5	30, 60, 90, 120, 150, 180

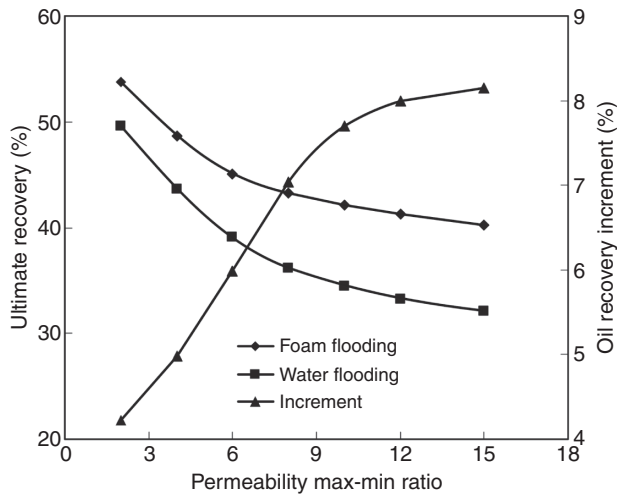


Figure 12
Ultimate recovery and increment vs permeability max-min ratio.

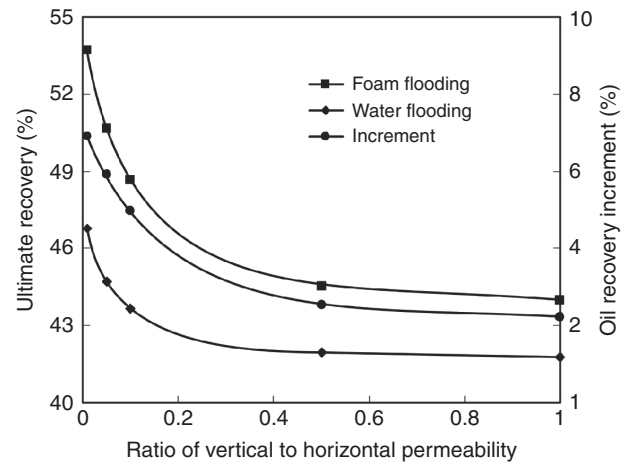


Figure 13
Ultimate recovery and the increment vs ratio of vertical to horizontal permeability.

quality and foaming agent concentration are very practical, common and important influencing factors in actual oilfields. Therefore, we performed a sensitivity analysis of these factors using the above heterogeneous reservoir and parameters. The parameters of the simulated projects are shown in Table 5.

3.2.1 Permeability Max-Min Ratio

The permeability max-min ratio is defined as the ratio of the highest permeability to the lowest permeability. Because foam has the feature of “big block and not small block”, if the reservoir has a suitable permeability max-min ratio, the EOR effect will be superior. Figure 12 shows the ultimate and incremental oil recoveries for different permeability max-min ratios. It is shown that when the permeability max-min ratio is small, the incremental oil recovery increases sharply as the ratio increases; when it reaches 10, the oil recovery increment reaches a plateau. The reason for this is the lower the permeability max-min ratio will result in the closer the permeability of each stratum. From Equation (10), the foam resistance factor is a function of permeability. For a smaller permeability max-min ratio reservoir, after foam flooding, the water diverting into the low-permeability layers is lowered; for a larger permeability max-min ratio reservoir, the foam resistance factor is larger in the high-permeability layer and more water diverts into the low-permeability layer to sweep the remaining oil. Due to the limited blocking capacity of foam, the foam strength decreases if the permeability is too large. Therefore, the ultimate recovery is not very good

for a reservoir with an extremely large permeability max-min ratio. Consequently, foam flooding is suitable for reservoirs with a moderate permeability max-min ratio.

3.2.2 Ratio of Vertical to Horizontal Permeability

Override is a problem in gas flooding. In gas flooding, the ratio of vertical to horizontal permeability should be considered. Figure 13 shows the ultimate and incremental oil recoveries for different ratios of vertical to horizontal permeability. It is shown that as the ratio of vertical to horizontal permeability increases, the incremental oil recovery sharply decreases. When the ratio is bigger than 0.2, the incremental oil recovery decreases slowly and is only about 2%. The reason is that if the ratio of vertical to horizontal permeability is large, the gas gravitational variations will be more pronounced. As a result, all the injected gas overrides into the top layer, and no foam is generated in the bottom layer. The continued water diversion would not take place. Therefore, foam flooding is suitable for reservoirs with a lower ratio of vertical to horizontal permeability.

The depositional sequence is defined as the regulation by which the sand particles deposit in sequence to form rock strata. A transgressive depositional sequence is composed of several sand layers where the sand diameter declines from the bottom to the top, *i.e.* the permeability is reduced in the vertical profile from the bottom to the top; a regressive depositional sequence is just the reverse. The depositional

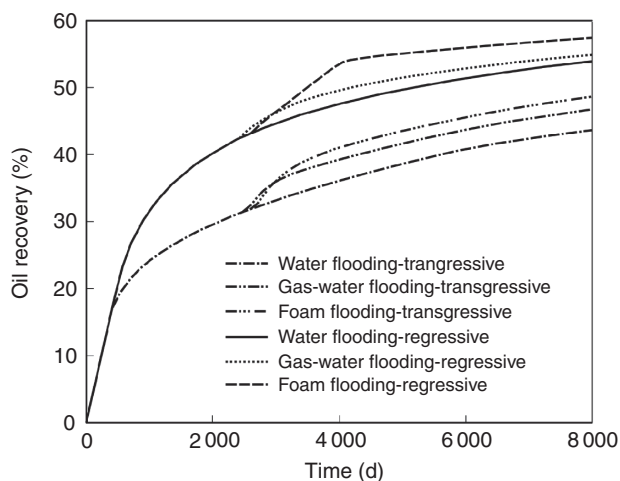


Figure 14

Comparison of the developments effects with different methods and depositional sequences.

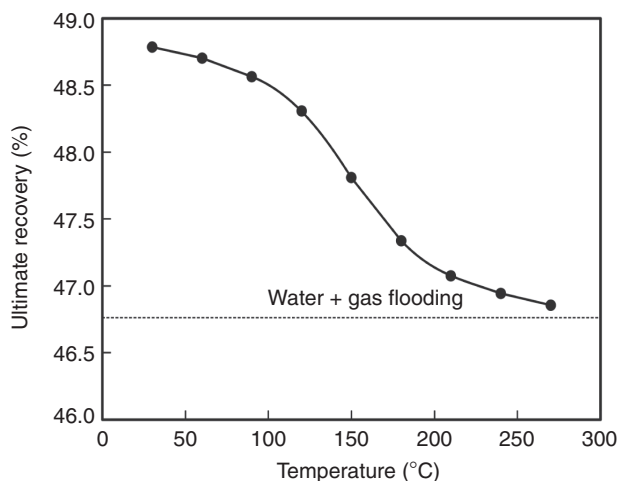


Figure 15

Ultimate recovery vs reservoir temperature.

sequence has a significant influence on the gas override to affect the ultimate recovery. Figure 14 shows the development effects with different displacing modes and depositional sequences. Apparently, the oil recovery in a regressive depositional sequence reservoir is higher than that in a transgressive depositional sequence reservoir for all the three displacing modes. The water + gas flooding oil recovery is higher than water flooding. However, the incremental oil recovery in regressive depositional sequence reservoirs is lower than transgressive depositional sequence reservoirs. The foam flooding oil recovery is higher than water + gas flooding. However, the incremental oil recovery in a regressive depositional sequence reservoir is higher than in a transgressive depositional sequence reservoir. For the rationale, in transgressive depositional sequence reservoirs, water is inclined to enter the high-permeability layer due to gravitational variations and lower flow resistance, which results in some remaining oil being confined within the low-permeability layer; continued gas is inclined to override into the low-permeability layer under the gravitational variations and displaces the remaining oil. In the regressive depositional sequence reservoirs, due to gravitational variations and lower flow resistance, both the high-permeability and low-permeability layers are well swept by water, and the remaining oil is lowered in the high-permeability layer (top layer); the gas is still inclined to enter the top layer due to gravitational variations and lower flow resistance, but the EOR effect is not obvious. Comparing foam flooding with water +

gas flooding, in the transgressive depositional sequence reservoirs, more gas flows in the low-permeability layers, and the amount of foam in high-permeability layers is less than regressive depositional sequence reservoirs, which results in less water diverting into lower-permeability layers after foam flooding. Conversely, in the regressive depositional sequence reservoirs, since more gas flows in the high-permeability layers, consequently, this results in more flow of foam in high-permeability layers as well. As a result, more water diverts into lower-permeability layers after foam flooding.

3.2.4 Reservoir Temperature

Figure 15 shows the variation of ultimate oil recovery with reservoir temperature. The ultimate oil recovery decreases as the temperature increases. When the temperature is lower than 100°C, the ultimate oil recovery varies very little; when the temperature is between 100 and 200°C, the ultimate oil recovery decreases sharply; when the temperature exceeds 200°C, the ultimate oil recovery of foam flooding is close to that of water + gas flooding. Therefore, the reservoir temperature should not be high, or temperature-tolerant foaming agents should be used for high-temperature reservoirs.

3.2.5 Foam Quality

Foam quality is an important factor determining the blocking capacity of the foam texture. Figure 16 shows the ultimate oil recovery of different foam qualities.

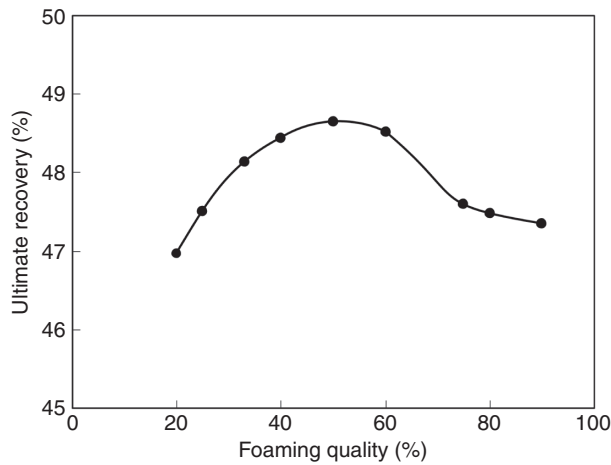


Figure 16
Ultimate recovery vs foam quality.

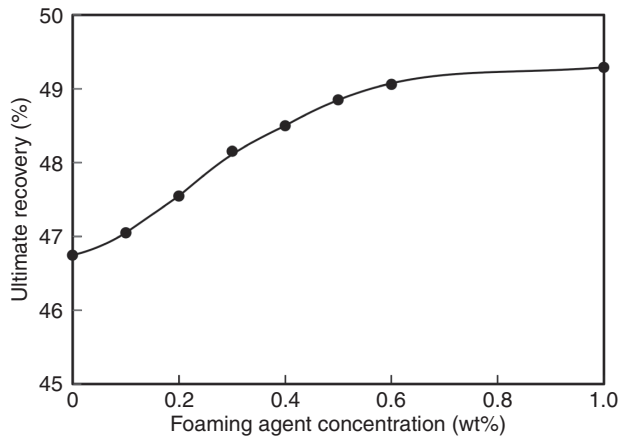


Figure 17
Ultimate recovery vs foaming agent concentration.

Evidently, as the foam quality increases, the ultimate oil recovery first increases and then decreases with an optimal value of 50%. This is due to the fact that a lower foam quality means a thicker lamella and a smaller bubble; under these conditions, the Jamin effect [51] is very small; conversely, a higher foam quality leads to a thinner lamella, a faster gas velocity and a bigger bubble; under these conditions, the bubble is more likely to collapse by shearing when it flows through the porous media. Therefore, a more stable bubble with a better Jamin effect can obtain a better EOR effect. Based on the relation between the foam quality and gas-water ratio, the optimal injection gas-water ratio should be chosen at the volume ratio of 1:1 under the reservoir conditions.

3.2.6 Foaming Agent Concentration

Figure 17 shows the variation of ultimate oil recovery with foaming agent concentration. Noticeably, the ultimate oil recovery reaches a plateau at 0.6 wt% after increasing along with the foaming agent concentration. Based on the parameters used in this case, the CMC is about 0.5 wt%. Optimal concentration is a little higher than the CMC since some of the foaming agent is adsorbed on the rock. So, the foaming agent concentration of foam flooding should be a little higher than the CMC of the surfactant.

CONCLUSIONS

A novel model of multi-factor foam flooding is established. The IMPES method in conjunction with a fourth-order Runge-Kutta method were used to solve the governing equation. The validation of this model was confirmed by matching the experimental data. Finally, the effects of several parameters including the permeability max-min ratio, ratio of vertical to horizontal permeability, depositional sequence, foam quality, foaming agent concentration, and reservoir temperature on oil recovery were studied. The following are the main conclusions:

- 1) A foam resistance factor model considering the influences of permeability, foaming agent concentration, foam quality, temperature and oil saturation is obtained. Then, taking the gas velocity as the foam generation condition and water saturation as the foam collapse condition, the gas mobility model was achieved;
- 2) Foam can effectively weaken the phenomena of gas override in the vertical direction due to gravitational variations and gas channeling in a horizontal direction caused by large gas mobility;
- 3) The mechanism of water + gas flooding enhanced oil recovery is that due to the gravitational variations, gas increases the swept area of the injected fluid; and the mechanisms of foam flooding are both the gravitational variations and the water diversion;
- 4) With a smaller permeability max-min ratio, the incremental oil recovery increases sharply and reaches a plateau at the ratio of 10. Foam flooding is suitable for reservoirs with a moderate permeability max-min ratio ($k_r = 5-10$);
- 5) As the ratio of vertical to horizontal permeability increases, the incremental oil recovery sharply decreases. When the ratio is bigger than 0.2, the incremental oil recovery decreases slowly, and is only about 2%. Foam flooding is appropriate for reservoirs whose ratio of vertical to horizontal permeability is lower than 0.2;

- 6) The oil recovery in regressive depositional sequence reservoirs is higher than that of transgressive depositional sequence reservoirs for water flooding, gas-water flooding and foam flooding. The gas-water flooding incremental oil recovery for water flooding in regressive depositional sequence reservoirs is less than that in transgressive depositional sequence reservoirs, but the foam flooding increment for water + gas flooding in regressive depositional sequence reservoirs is more than that in transgressive depositional sequence reservoirs;
- 7) The ultimate recovery decreases as the temperature increases. The reservoir temperature should not be high for foam flooding; otherwise, temperature-tolerant foaming agents should be used for high-temperature reservoirs;
- 8) As the foam quality increases, the ultimate oil recovery first increases and then decreases, and the optimal value is 50%. The optimal injection for the gas-water ratio should be chosen at the volume ratio of 1:1 under the reservoir conditions;
- 9) Due to adsorption of the surfactant, the foaming agent concentration during foam flooding should be a little higher than the CMC of the surfactant.

ACKNOWLEDGMENTS

This study was funded by the Chinese National Natural Science Foundation (51274212) and Important National Science & Technology Specific Projects of China (2011ZX05014-003-008HZ).

REFERENCES

- 1 Casteel J.F., Djabbarah N.F. (1988) Sweep Improvement in CO₂ Flooding by Use of Foaming Agents, *SPE Reserv. Eng.* **3**, 4, 1186-1192.
- 2 Namdar Z.M., Kam S.I., LaForce T.C., Rossen W.R. (2011) The Method of Characteristics Applied to Oil Displacement by Foam, *SPE J.* **16**, 1, 8-23.
- 3 Yang H., Yue X.A., Zhao R.B., Yang Z.P. (2009) Experimental Study on Validity of Foam Plugging in Porous Media, *Oilfield Chemistry* **3**, 273-275.
- 4 Zhu Y.Y., Hou Q.F., Weng R., Jian G.Q., Luo Y.S., Li J.G. (2013) Recent Progress and Effects Analysis of Foam Flooding Field Tests in China, *SPE paper* 165211 presented at 2013 *SPE Enhanced Oil Recovery Conference*, Kuala Lumpur, Malaysia, 02-04 July.
- 5 Kovscek A.R., Patzek T.W., Radke C.J. (1994) Mechanistic Prediction of Foam Displacement in Multidimensions: A Population Balance Approach, *SPE paper* 27789 presented at 1994 *SPE/DOE Improved Oil Recovery Symposium*, Tulsa, Oklahoma, 17-20 April.

- 6 Rossen W.R., Zeilinger S.C., Shi J.X., Lim M.T. (1999) Simplified Mechanistic Simulation of Foam Processes in Porous Media, *SPE J.* **4**, 3, 279-287.
- 7 Kovscek A.R., Bertin H.J. (2002) Estimation of Foam Mobility in Heterogeneous Porous Media, *SPE paper* 75181 presented at 2002 *SPE/DOE Improved Oil Recovery Symposium*, Tulsa, Oklahoma, 13-17 April.
- 8 Du Q.J. (2008) Experiment and Modeling of the Seepage Characteristics in Foam Flooding. A *Dissertation* Submitted for the Degree of Doctor of Philosophy of China University of Petroleum, Shandong, China.
- 9 Han D.K. (1993) *Numerical Reservoir Simulation*, Petroleum Industry Press, Beijing, China.
- 10 Falls A.H., Musters J.J., Ratulowski J. (1989) The Apparent Viscosity of Foams in Homogeneous Bead packs, *SPE Reserv. Eng.* **4**, 2, 155-164.
- 11 Chang S.H., Owusu L.A., French S.B., Kovarik F.S. (1990) The Effect of Microscopic Heterogeneity on CO₂-Foam Mobility: Part 2 - Mechanistic Foam Simulation, *SPE paper* 20191 presented at 1990 *Seventh Symposium on Enhanced Oil Recovery*, Tulsa, Oklahoma, 22-25 April.
- 12 Friedmann F., Chen W.H., Gauglitz P.A. (1991) Experimental and Simulation Study of High-Temperature Foam Displacement in Porous Media, *SPE Reserv. Eng.* **6**, 1, 37-45.
- 13 Kovscek A.R., Patzek T.W., Radke C.J. (1993) Simulation of Foam Transport in Porous Media, *SPE paper* 26402 presented at 1993 *SPE Annual Technical Conference and Exhibition*, Houston, Texas, 3-6 Oct.
- 14 Low D.H.S., Yang Z.M., Stone T.W. (1992) Effect of the Presence of Oil on Foam Performance: A Field Simulation Study, *SPE Reserv. Eng.* **7**, 2, 228-236.
- 15 Patzek T.W., Myhill N.A. (1989) Simulation of The Bishop Steam Foam Pilot, *SPE paper* 18786 presented at 1989 *SPE California Regional Meeting*, Bakersfield, 5-7 April.
- 16 Kular G.S., Lowe K., Coombe D. (1989) Foam Application in an Oil Sands Steam Flood Process, *SPE paper* 19690 presented at 1989 *SPE Annual Tech. Conf. and Exhibition*, San Antonio, Texas, 8-11 Oct.
- 17 Islam M.R., Farouq-Ali S.M. (1990) Numerical Simulation of Foam Flow in Porous Media, *J. Can. Pet. Tech.* **29**, 4, 47-51.
- 18 Rossen W.R., Zhou Z.H., Mamun, C.K. (1991) Modeling Foam Mobility at "The Limiting Capillary Pressure", *SPE paper* 22627 presented at 1991 *Annual Tech. Conf. and Exhibition*, Dallas, Texas, 6-9 Oct.
- 19 Khatib Z.I., Hirasaki G.J., Falls A.H. (1988) Effects of Capillary Pressure on Coalescence and Phase Mobilities in Foams Flowing through Porous Media, *SPE Reserv. Eng.* **3**, 3, 919-926.
- 20 Wang J., Liu H.Q., Ning Z.F., Zhang H.L. (2012) Experimental Research and Quantitative Characterization of Nitrogen Foam Blocking Characteristics, *Energy & Fuels* **26**, 8, 5152-5163.
- 21 <http://www.oakdaleengr.com/index.html>.
- 22 De Vries A.S., Wit K. (1990) Rheology of Gas/water Foam in The Quality Range Relevant to Steam Foam, *SPE Reserv. Eng.* **5**, 2, 185-192.
- 23 Chang S.H., Grigg R.B. (1996) Foam Displacement Modeling in CO₂ Flooding Processes, *SPE paper* 35401 presented at 1996 *SPE/DOE Improved Oil Recovery Symposium*, Tulsa, Oklahoma, 21-24 April.
- 24 Isaacs E.E., McCarthy F.C., Maunder J.D. (1988) Investigation of Foam Stability in Porous Media at Elevated Temperatures, *SPE Reserv. Eng.* **3**, 2, 565-572.

- 25 Xu Q., Rossen W.R. (2003) Effective Viscosity of Foam in Periodically Constricted Tubes, *Colloids Surf. A.* **216**, 1-3, 175-194.
- 26 Cox S.J., Neethling S., Rossen W.R., Schleifenbaum W., Schmidt-Wellenburg P., Cilliers J.J. (2004) A Theory of The Effective Yield Stress of Foam in Porous Media: The Motion of A Soap Film Traversing A Three-Dimensional Pore, *Colloids Surf. A.* **245**, 1-3, 143-151.
- 27 Wang Z., Ganesan N. (2006) Model for Plateau Border Drainage of Power-Law Fluid with Mobile Interface and Its Application to Foam Drainage, *J. Colloid Interface Sci.* **300**, 1, 327-337.
- 28 Pacelli L.J., Quoc P.N., Peter K.C., Marten A.B. (2006) Coupling of Foam Drainage and Viscous Fingering in Porous Media Revealed by X-ray Computed Tomography, *Transp. Porous Med.* **64**, 3, 301-313.
- 29 Muijs H.M., Keijzer P.P.M., Wiersma R.J. (1988) Surfactants for Mobility Control in High-Temperature Steam-Foam Applications, *SPE paper 17361* presented at 1988 *SPE Enhanced Oil Recovery Symposium*, Tulsa, Oklahoma, 16-21, April.
- 30 Maini B.B., Ma V. (1986) Laboratory Evaluation of Foaming Agents for High-Temperature Applications - I. Measurements of Foam Stability at Elevated Temperatures and Pressures, *J. Can. Petrol. Tech.* **25**, 6, 65-69.
- 31 Nikolov A.D., Wasan D.T., Huang D.W., Edwards D.A. (1986) The Effect of Oil on Foam Stability: Mechanisms and Implications for Oil Displacement by Foam in Porous Media, *SPE paper 15443* presented at 1986 *SPE Annual Technical Conference and Exhibition*, New Orleans, Louisiana, 5-8 Oct.
- 32 Suffridge F.E., Raterman K.T., Russell G.C. (1989) Foam Performance under Reservoir Conditions, *SPE paper 19691* presented at 1989 *SPE Annual Technical Conference and Exhibition*, San Antonio, Texas, 8-11 Oct.
- 33 Emadi A., Sohrabi M., Jamiolahmady M., Ireland S., Robertson G. (2011) Mechanistic Study of Improved Heavy Oil Recovery by CO₂-Foam Injection, *SPE paper 143013* presented at *SPE Enhanced Oil Recovery Conference*, Kuala Lumpur, Malaysia, 19-21 July.
- 34 Andrianov A., Farajzadeh R., Mahmoodi N.M., Talanana M., Zitha P.L.J. (2012) Immiscible Foam for Enhancing Oil Recovery: Bulk and Porous Media Experiments, *Ind. Eng. Chem. Res.* **51**, 5, 2214-2226.
- 35 Jensen J.A., Friedmann F. (1987) Physical and Chemical Effects of an Oil Phase on the Propagation of Foam in Porous Media, *SPE paper 14375* presented at 1987 *SPE California Regional Meeting*, Ventura, California, 8-10 April.
- 36 Svorstøl I., Vassenden F., Mannhardt K. (1996) Laboratory Studies for Design of a Foam Pilot in the Snorre Field, *SPE paper 35400* presented at 1996 *SPE/DOE Improved Oil Recovery Symposium*, Tulsa, Oklahoma, 21-24 April.
- 37 Mannhardt K., Svorstøl I. (1999) Effect of Oil Saturation on Foam Propagation in Snorre Reservoir Core, *J. Pet. Sci. Eng.* **23**, 3-4, 189-200.
- 38 Farajzadeh R., Andrianov A., Krastev R., Hirasaki G.J., Rossen W.R. (2012) Foam-Oil Interaction in Porous Media: Implications for Foam Assisted Enhanced Oil Recovery, *SPE paper 154197* presented at 2012 *SPE EOR Conference at Oil and Gas West Asia*, Muscat, Oman, 16-18 April.
- 39 Simjoo M., Dong Y.F., Andrianov A., Talanana M., Zitha P.L.J. (2012) Novel Insight into Foam Mobility Control, *SPE paper 15338* presented at 2012 *International Petroleum Technology Conference*, Bangkok, Thailand, 7-9 Feb.
- 40 Arnaudov L., Denkov N.D., Surcheva I., Durbut P., Broze G., Mehreteab A. (2001) Effect of Oily Additives on Foam Ability and Foam Stability. 1. Role of Interfacial Properties, *Langmuir* **17**, 22, 6999-7010.
- 41 Derjaguin B., Landau L. (1941) Theory of the Stability of Strongly Charged Lyophobic Sols and of the Adhesion of Strongly Charged Particles in Solutions of Electrolytes, *Acta Physico Chemica URSS* **14**, 633-662.
- 42 Verwey E.J.W., Overbeek J.Th.G. (1948) *Theory of the Stability of Lyophobic Colloids*, Elsevier, Amsterdam.
- 43 Shi J.X., Rossen W.R. (1998) Simulation and Dimensional Analysis of Foam Processes in Porous Media, *SPE Reserv. Eval. Eng.* **1**, 2, 148-154.
- 44 Kovscek A.R., Patzek T.W., Radke C.J. (1997) Mechanistic Foam Flow Simulation in Heterogeneous and Multidimensional Porous Media, *SPE J.* **2**, 4, 511-526.
- 45 Yu H.M., Ren S.R., Zuo J.L. (2012) A Mathematical Model and Numerical Simulation Method for Air-Foam, *Acta Petrolei Sinica* **33**, 4, 653-657.
- 46 Hou J., Du Q.J., Li Z.Q., Pan G.M., Lu X.J., Zhou K. (2013) Experiments on Foam Texture under High Pressure in Porous Media, *Flow Measurement and Instrumentation* **33**, 68-76.
- 47 Simjoo M., Rezaei T., Andrianov A., Zitha P.L.J. (2013) Foam Stability in the Presence of Oil: Effect of Surfactant Concentration and Oil Type, *Colloids and Surfaces A: Physicochemical and Engineering Aspects* **438**, 148-158.
- 48 Stone H.L. (1973) Estimation of Three-Phase Relative Permeability and Residual Oil Data, *J. Can. Pet. Tech.* **12**, 4, 53-61.
- 49 Qin J.S., Li A.F. (2001) *Petrophysics*, China University of Petroleum Press, Shandong, China.
- 50 Poston S.W., Gross S.J. (1986) Numerical Simulation of Sandstone Reservoir Models, *SPE Reservoir Engineering* **1**, 4, 423-429.
- 51 Wright R. (1933) Jamin Effect in Oil Production, *AAPG Bulletin* **17**, 12, 1521-1526.

Manuscript accepted in April 2014

Published online in July 2014